Reliable Modeling for Safe Navigation of Intelligent Vehicles: Analysis of First and Second Order Set-membership TTC

Nadhir Mansour Ben Lakhal[1,2], Othman Nasri[2], Lounis Adouane[3] and Jaleleddine Ben Hadj Slama[2]
[1]*Institut Pascal, UCA/SIGMA - UMR CNRS 6602, Clermont Auvergne University, France*
[2]*LATIS Lab, National Engineering School of Sousse (ENISo), University of Sousse, BP 264 Sousse Erriadh 1023, Tunisia*
[3]*Heudiasyc UMR CNRS/UTC 7253, Université de Technologie de Compiègne, 60203 Compiègne, France*

Keywords: Intelligent Vehicles, Risk Management, Interval-based Modeling, Correlation Analysis, Interval Polynomial, Second-order Time to Collision.

Abstract: Developing high fidelity models to compute the Time-To-Collision (TTC) between vehicles is addressed in this work. A TTC interval value is over-approximated while considering several uncertainties via interval analysis. Furthermore, to decrease modeling inaccuracy, a novel second-order set-membership TTC formalization is introduced by solving a polynomial equation with interval coefficients. This latter is derived from vehicles' motion equations. Hence, an approach based on correlation analysis is exploited to improve the uncertainty evaluation. The simulation results applied on an adaptive cruise control system of both high/low-order TTC formalizations prove that the low-order model inaccuracy is compensated. Thanks to interval analysis and correlation characterization, a great balance between modeling accuracy and simplicity is reached.

1 INTRODUCTION

Risk management should be inspected carefully to employ autonomous vehicles in public roads (Nasri et al., 2019). For the sake of safety, focus is currently given to provide efficient solutions for in-road risk identification. Thus, factors that stand behind the reliability and accuracy of safety verification techniques should be analyzed.

Advanced perception/communication devices and navigation scene analysis have been used to capture in-road hazards (Abdi and Meddeb, 2018), (Kasmi et al., 2019). Nonetheless, these tools are prone to severe uncertainties. To overcome uncertainty impacts, several methods have been proposed in the literature (Lakhal et al., 2019a), (Lozenguez et al., 2011). The uncertainty is propagated into the navigation process via stochastic models such as the Kalman filter, etc. A specific probability distribution, as the Gaussian function, is assumed to describe the uncertainty evolution. This assumption is controversial, and changes in noise features may occur (Rigatos, 2012). Additionally, most uncertainty evolution models are sensitive to non-linearity (Wang et al., 2018). On top of that, an accurate knowledge of the initial states of the studied system is required, which is not evident (Nicola and Jaulin, 2018). Hence, it is important to study alternative approaches that are less sensitive to these errors.

Otherwise, risk management reliability depends on the accuracy of models used to derive numerous risk indicators. For instance, the Time To Collision (TTC) has been widely used for risk identification (Iberraken et al., 2018), (Iberraken et al., 2019). Tremendous attempts have been made to improve the TTC precision. A comparative study between diverse TTC formalizations could be found in (Hou et al., 2014). A hidden Markov model has been used to predict the driving intention of nearby vehicles for more accurate TTC estimation (Yang et al., 2020). Algorithms computing distances between boxes bounding vehicles were proposed to calculate TTC for complex traffic scenarios (Wang et al., 2018). A vehicle motion-based concept, named looming, was exploited to decrease the TTC false alarms (Ward et al., 2015).

Interval analysis is a reliable way to handle uncertainties/modeling imperfections (Jaulin et al., 2001). It turns standard data to intervals to bound uncertainty impacting the studied system (Moore et al., 2009). Correspondingly, interval analysis may contribute strongly in characterizing the uncertainty evolution into intelligent transportation systems. In previous work, an interval-based model to compute TTC for a car-following scenario was proposed to handle

Ben Lakhal, N., Nasri, O., Adouane, L. and Slama, J.
Reliable Modeling for Safe Navigation of Intelligent Vehicles: Analysis of First and Second Order Set-membership TTC.
DOI: 10.5220/0009890305450552
In *Proceedings of the 17th International Conference on Informatics in Control, Automation and Robotics (ICINCO 2020)*, pages 545-552
ISBN: 978-989-758-442-8

uncertainties and communication latencies (Lakhal et al., 2019b) and (Lakhal et al., 2019c). Moreover, the interval TTC over-approximation was optimized via a data-driven characterization of correlation that would relate the navigation system variables. In this paper, we build on this previous work to analyze much comprehensively the performances of the set-membership modeling. The main contribution of this work is to introduce a novel second-order interval-based TTC over-approximation to consider more parameters intervening in the car-following scenario. The high-order model consists in a quadratic polynomial with interval coefficients generated from vehicles' motion equations. Usually dedicated to bound the rounding errors, interval polynomials have never been used to build models for uncertainty evolution into navigation systems. Afterwards, simulation is elaborated on an Adaptive Cruise Control (ACC). The performances of the interval high and low-order TTC in conducting the risk worst-case analysis are compared. The quality of the set-membership modeling joined with the correlation analysis is evaluated in terms of accuracy and simplicity.

The rest of this paper is arranged as follows: Section 2 introduces the first and second-order TTC interval-based formalizations. Section 3 presents an algorithm to find roots for an interval polynomial to approximate the TTC. Section 4 explains the correlation analysis role in ameliorating the findings of the TTC set-membership models. Section 5 presents the simulation results. Section 6 concludes the results of this work and discusses some future work.

2 SECOND ORDER SET-MEMBERSHIP TTC

For a car-following scenario, the TTC is often approximated by the ratio between the distance separating two vehicles and their relative velocity. Instead, the evolution of the spacing distance between the follower and the leader is used in this paper to perform more accurate collision prediction. In this way, all the interactions between vehicles are taken into account. Let consider two vehicles i and j, which are respectively the leader and the follower. V_i, V_j, p_i and p_j are their respective velocities and vector positions. According to (Ward et al., 2015), the separation evolution between both vehicles is described at each instant by:

- The separation distance:

$$d_{ij} = \sqrt{(p_i - p_j)^T (p_i - p_j)} \tag{1}$$

- The change rate in the separation distance:

$$\dot{d}_{ij} = \frac{1}{d_{ij}} (p_i - p_j)^T (V_i - V_j) \tag{2}$$

- The variation of the change rate in the separation distance is governed by the following equation:

$$\ddot{d}_{ij} = \frac{1}{d_{ij}} (V_i - V_j)^T (V_i - V_j) - \dot{d}_{ij}^2 \tag{3}$$

Equations (2) and (3) are obtained by the consecutive differentiation of equation (1). In practice, d_{ij} is measured in run-time thanks to diverse vehicular tools as a LiDAR or laser scanner. Therefore, the authors in (Ward et al., 2015) defined TTC_1 as a first order TTC:

$$TTC_1 = -\frac{d_{ij}}{\dot{d}_{ij}} \tag{4}$$

However, equation (4) neglects parameter $\ddot{d}_{ij}$. Model simplification is the main source of errors (Khelifi et al., 2018). In an effort to improve accuracy, the authors in (Ward et al., 2015) upgraded the TTC approximation to a second-order expression. When $\ddot{d}_{ij} \neq 0$, a second-order TTC, denoted TTC_2, is obtained by solving the following polynomial:

$$d_{ij} + \dot{d}_{ij} TTC_2 + \frac{1}{2} \ddot{d}_{ij} TTC_2^2 = 0 \tag{5}$$

Note that equation (5) is derived from the vehicles' motion equations. The polynomial roots underline at which instants the two vehicles collide, and the separation between them is zero. Accordingly, the authors in (Ward et al., 2015) defined the TTC_2 value depending on the roots of equation (5). When $\ddot{d}_{ij} = 0$ or the polynomial has no real roots, the low-order model is used and $TTC_2 = TTC_1$. In the case of two real positive roots, the lower value is attributed to TTC_2 since it presents the first collision time. If one of the roots is positive and the other is negative, the positive one is taken. Both roots can be also negative. In such a situation, the root with the closest absolute value to zero is selected because it consists of the most recent interaction between the motions of both vehicles.

Despite its accuracy, the high-order TTC is still sensitive to uncertainty and communication latencies. To overcome this issue, interval analysis is adopted in this paper. Data representation is extended to intervals. Mathematical operations $(+, -, *, /)$ and functions $(sin, cos, etc.)$ are extended to handle intervals (Jaulin et al., 2001). Subsequently, the obtained interval-based models provide over-approximations of results that definitely enclose the exact outputs. Henceforth, $[x] = [\underline{x}, \overline{x}]$ is a real interval, where $\underline{x}$ and $\overline{x}$ are its lower and upper bounds. The width of $[x]$

underlines the uncertainty extent. Accordingly, equations (4) and (5) are represented as:

$$[TTC_1] = -\frac{[d_{ij}]}{[\dot{d}_{ij}]} \tag{6}$$

$$[d_{ij}] + [\dot{d}_{ij}][TTC_2] + \frac{1}{2}[\ddot{d}_{ij}][TTC_2]^2 = 0 \tag{7}$$

Since it describes the real behavior, the second-order set-membership TTC is expected to be more accurate than the first-order one. Equation (7) is a quadratic polynomial with perturbed coefficients. Its roots are intervals enclosing the collision exact time. Solving this polynomial is not feasible by standard analytical approaches. A specific interval polynomial solver must be used. Before doing so, a methodological manner to quantify uncertainties attributed to each interval measurement is introduced. The environmental circumstances, where more uncertainties are expected, are examined. At first, the following assumptions, which are based on the confidence intervals of sensors and communication devices, are admitted:

- The localization inaccuracy is assessed via a signal strength indicator that considers the signal attenuation in the navigation zone.
- The accumulated error impacting the separation distance measurement is considered by an uncertainty range of $\pm 1\%$ from the measured d_{ij}.
- The follower speed V_j is assumed to be exact, and no uncertainty is attributed to this parameter.
- The leader speed V_i is assumed to be erroneous with a range of $\pm 0.5\%$ due to measurement imprecision.

Afterwards, several latencies can slow down the automotive system operation and prohibit the quick management of risks. For that reason, it is advisable to consider such latencies by $[TTC]$. In this work, the follower car is expected to receive the V_i value via a Vehicle-to-Vehicle (V2V) communication. Henceforth, latencies impacting the V2V communication are characterized through interval $[T_{V2V}]$. The uncertainty attributed to $[T_{V2V}]$ is appraised through the empirical research work depicted in (Dey et al., 2016). Min/max values of latencies that may happen were provided in (Dey et al., 2016). These bounds were presented as a function of the vehicle speed and the number of connected vehicles in close proximity (communication conflicts increase delays). Besides, $[T_L]$ is a constant interval that takes into account latencies due to update time of sensors and the data propagation into the embedded system. Consequently, the TTC set-membership formalization must consider explicitly the aforementioned uncertainty sources:

$$[TTC_1] = -\frac{[d_{ij}]}{[\dot{d}_{ij}]} - [T_{V2V}] - [T_L] \tag{8}$$

$$[TTC_2] = [\Re] - [T_{V2V}] - [T_L] \tag{9}$$

where $[\Re]$ is the polynomial root of equation (7). Similar to the deterministic case detailed above (cf. equation (5)), $[\Re]$ is the root corresponding to the first collision time. Figure 1 illustrates the main instructions of the proposed uncertainty quantification strategy to over-approximate the first/second order TTC.

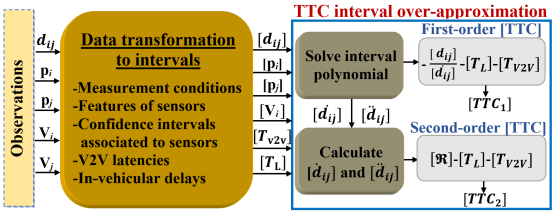

Figure 1: Interval-based risk management.

3 SOLVING QUADRATIC INTERVAL POLYNOMIAL

Finding roots for interval polynomials has been widely discussed in the literature. Several numerical branch and bound algorithms were introduced for this aim (Fan et al., 2008). Despite their accuracy, the calculation time of these approaches was unpredictable. One more category of approaches used polynomial factorization and cumbersome mathematical calculation as an inverting interval matrix (Zhang and Deng, 2013). Other fast methods were developed (Ferreira et al., 2001). Nevertheless, these approaches provided just a prior estimate for the space containing the real roots. In this work, real roots with sharp bounds of interval polynomials are obtained by studying the interval polynomial boundary functions.

Let consider a quadratic polynomial with the following shape:

$$P([x]) = [a]x^2 + [b]x + [c] \tag{10}$$

Intuitively, $P([x])$ can be expressed within its boundary functions, where: $P([x]) = [\underline{P}([x]), \overline{P}([x])]$. For such a polynomial, $\underline{P}([x])$ and $\overline{P}([x])$ may be derived through all possible combinations between the coefficient bounds. Indeed, eight real single-valued polynomials are given from these combinations:

$$\begin{cases} f_1 = \underline{a}x^2 + \underline{b}x + \underline{c}; & f_2 = \underline{a}x^2 + \underline{b}x + \overline{c} \\ f_3 = \underline{a}x^2 + \overline{b}x + \underline{c}; & f_4 = \underline{a}x^2 + \overline{b}x + \overline{c} \\ f_5 = \overline{a}x^2 + \underline{b}x + \underline{c}; & f_6 = \overline{a}x^2 + \underline{b}x + \overline{c} \\ f_7 = \overline{a}x^2 + \overline{b}x + \underline{c}; & f_8 = \overline{a}x^2 + \overline{b}x + \overline{c} \end{cases} \tag{11}$$

By interpreting the dominant term of $P([x])$, it is evident that $\underline{P}([x])$ and $\overline{P}([x])$ are respectively enclosed between (f_1, f_2, f_3, f_4) and (f_5, f_6, f_7, f_8). It is clear also that:

$$\begin{cases} f_1 \leq f_2; & f_3 \leq f_4 \\ f_6 \geq f_5; & f_7 \geq f_8 \end{cases} \tag{12}$$

Subsequently, we can figure out that:

$$\underline{P(x)} = \begin{cases} P_1 = \underline{a}x^2 + \underline{b}x + \underline{c}, & \text{if } x \geq 0 \\ P_2 = \underline{a}x^2 + \overline{b}x + \underline{c}, & \text{if } x \leq 0 \end{cases} \tag{13}$$

and

$$\overline{P(x)} = \begin{cases} P_3 = \overline{a}x^2 + \overline{b}x + \overline{c}, & \text{if } x \geq 0 \\ P_4 = \overline{a}x^2 + \underline{b}x + \overline{c}, & \text{if } x \leq 0 \end{cases} \tag{14}$$

Note that $P_{i=1..4} = (P_1, P_2, P_3, P_4)$ represents non-interval real boundary functions associated to $P([x])$. To illustrate such a notion, Figure 2 presents two examples of quadratic polynomials with perturbed coefficients.

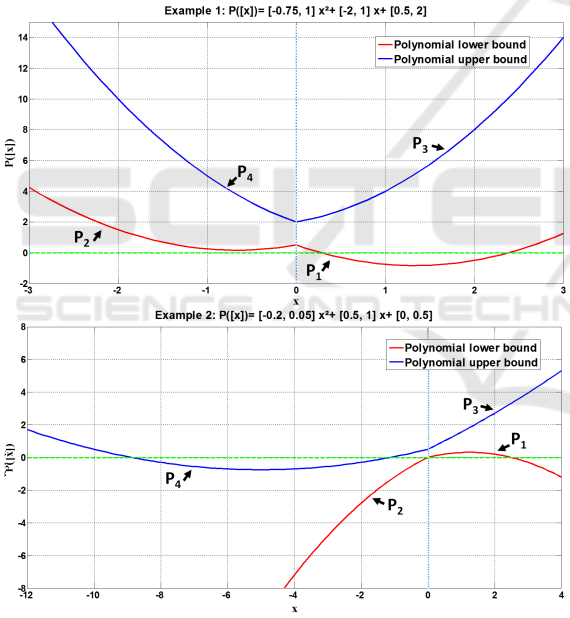

Figure 2: Examples of interval polynomials.

An efficient way to find polynomial roots is to determine sets where: $\underline{P}([x]) \leq 0 \leq \overline{P}([x])$. Eventually, estimating sharp bounds of this intersection should be accomplished by solving $P_{i=1..4}$. Once the roots of the boundary functions $P_{i=1..4}$ are calculated, it remains to clarify how to join these roots to formulate a precise enclosure of $P([x])$ solutions. Contrary to non-interval polynomials, $P([x])$ may have at maximum three distinct interval roots, including semi-infinite intervals (see Figure 2).

In this work, a simple algorithm is presented to extract $P([x])$ interval roots using $P_{i=1..4}$. It is based on the theoretical results obtained in (Hansen and Walster, 2002) and (Hansen and Walster, 2003), where the $P([x])$ coefficient bounds are analyzed to figure out the shape and orientation of $\underline{P}(x)$ and $\overline{P}(x)$. Consequently, the right number and values of the interval roots are appropriately determined.

First, the number of subcases that must be checked to resolve $P([x])$ is decreased by admitting $\overline{a} > 0$. In the opposite case, the sign of $P([x])$ must be simply reversed. Therefore, each P_i must be solved by interval arithmetic. The readers must distinguish between solving interval polynomials and isolating real roots of standard polynomials. Several set-membership algorithms resolve the non-interval polynomials in order to bound rounding errors.

In this work, the real roots of $P_{i=1..4}$ are computed numerically via a specific interval computation package. The isolated real roots associated to each P_i, including multiple roots, are added to list L. Since functions P_1 and P_2 bound $P([x])$ only for $x \geq 0$ (see equation (13)), any negative root or part of a root must indefinitely be discarded from L. Seemingly, positive roots or parts of roots associated to P_3 and P_4 are dropped.

Otherwise, there are some particular cases that must be considered while arranging L. Indeed, a double root is obtained at $x = 0$ for (P_1, P_2) when $\underline{c} = 0$ and respectively for (P_3, P_4) if $\overline{c} = 0$. For both cases, this root must be entered just one time into the list. Besides, the infinite interval endpoints $\pm\infty$ must be placed if necessary in L. Referring to (Hansen and Walster, 2003), once the following cases are satisfied, a lower endpoint $-\infty$ is added to L :

$$\underline{a} < 0 \vee (\underline{a} = 0 \wedge \overline{b} > 0) \vee (\underline{a} = 0 \wedge \overline{b} = 0 \wedge \underline{c} \leq 0) \tag{15}$$

Likewise, $+\infty$ is added to L only if:

$$\underline{a} < 0 \vee (\underline{a} = 0 \wedge \underline{b} > 0) \vee (\underline{a} = 0 \wedge \underline{b} = 0 \wedge \underline{c} \leq 0) \tag{16}$$

At this stage, L contains intervals that certainly present a lower or upper end-point of the final interval roots of $P([x])$. Thus, it is necessary to recognize which are the lower and upper ones. Let denote $[S_i] = [\underline{S_i}, \overline{S_i}]$ the set of intervals held in L. All intervals $[S_i]$ are sorted such that $\underline{S_i} \leq \underline{S_{i+1}}$. It is worth mentioning that the adopted algorithm requires to consider $\pm\infty$ as degenerate intervals. Hence, n denotes the number of intervals included in L (no more than six roots $0 \leq n \leq 6$). The final step from the root finding strategy consists in arranging the solution according to the obtained n. Table 1 summarizes all probable shapes of the interval roots associated to $P([x])$. Finally, all necessary steps to solve the interval polynomial are recapitulated in Algorithm 1.

Table 1: Interval roots according to n.

	Interval roots
$n=0$	$\varnothing$
$n=2$	$[\underline{S_1},\overline{S_2}]$
$n=4$	$[\underline{S_1},\overline{S_2}],[\underline{S_3},\overline{S_4}]$
$n=6$	$[-\infty,\overline{S_2}],[\underline{S_3},\overline{S_4}],[\underline{S_5},+\infty]$

Algorithm 1: Solving Interval Polynomial.

Require: $[a]$, $[b]$ and $[c]$
Ensure : Solve $P([x])=[a]x^2+[b]x+[c]$

1 *-Define $P_{i=1..4}$ (cf. equations (12) and (13)).*
2 *-Find interval roots of $P_{i=1..4}$.*
3 *-Put results in L.*
4 *-Add infinite entries $\pm\infty$ to L, if needed (cf. equations (15) and (16)).*
5 *-Sort the interval elements in L ($\underline{S_i} \leq \underline{S_{i+1}}$).*
6 *-Check the length of L to define roots of $P([x])$.*

4 CORRELATION-BASED OPTIMIZATION STEP

In this work, the interval-based TTC formalizations are dedicated to ensure safety for a modern ACC system. At every sample time, an interval enclosure for the position of target assigned to the ACC-equipped vehicle (follower) is defined proportionally to the current $[TTC]$, which is calculated via the first or second-order formalization. Then, a reference distance, denoted d_{ref}, is maintained from the in-front vehicle according to the worst-case risk indicated by the target enclosure (cf. Figure 3).

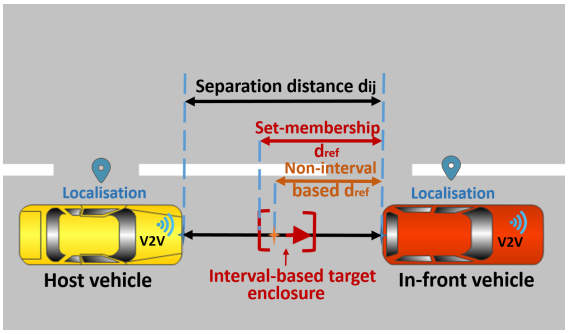

Figure 3: Proposed ACC risk management principle.

Nevertheless, the interval over-approximations obtained through assumptions defined in section 2 are too conservative. The occurrence of the worst cases of uncertainties for all parameters considered in the TTC computation is quite unrealistic. The main task of ACC systems is to optimize the distance between vehicles to prevent congestion and traffic disturbances. In this sense, the model developed for risk identification must make a trade off between safety and accuracy. As an enhancement for the interval-based models, a data-driven optimization step was introduced in the previous work of (Lakhal et al., 2019b), (Lakhal et al., 2019c) and (Ben Lakhel et al., 2016). Accordingly, this approach is joined to the TTC second-order model to obtain more compact bounds of findings. In this section, the proposed data-driven optimization approach is briefly recalled.

Correlation is a relevant statistical parameter to describe the operation of systems. More focus is given currently to correlation analysis to study the performances of autonomous vehicles (Wu et al., 2020). The main idea behind the proposed data-driven-optimization step is to examine the correlation progression over time. During the navigation runtime, substantial and brutal changes in vehicle dynamics are unrealistic in few sampling periods. Based on this understanding, the evolution of the correlation states should be smooth. Only uncertainties and erroneous measurements may invoke an irregular progression of correlation. Various data-driven approaches have relied on this assumption to capture faults or to regress outliers (Xia et al., 2017), (Chen et al., 2019).

Uncertainties assigned to interval measurements can be over-estimated. This fact may entail a brutal variation in the correlation progression between two successive instants: t_{k-1} and t_k. Hence, the proposed approach narrows recursively intervals until obtaining an acceptable progression in the correlation between variables. Narrowing is interpreted once the correlation relating the new tightened intervals matches reference values characterized off-line. Let denote by $C_{([X],[Y])|k}$ the correlation relating interval variables $[X]$ and $[Y]$ at instant t_k. The overall process to estimate the correlation values for interval variables is detailed in (Lakhal et al., 2019b). Thereafter, the gap in the correlation between instants t_k and t_{k-1}, denoted $\gamma_{k|k-1}$, is estimated through equation (17):

$$\gamma_{k|k-1} = C_{([X],[Y])|k} - C_{([X],[Y])|k-1} \qquad (17)$$

Interval widths must be narrowed in a recursive way to adapt the value of $\gamma_{k|k-1}$ in run-time and eliminate over-estimated uncertainties. For each couple of interval-valued variables intervening in the TTC computation, the interval with the largest width is concerned with iterative narrowing. After that, narrowing is aborted at two conditions:

- **Condition 1.** When $\gamma_{k|k-1}$ decreases from one iteration to another and suddenly starts to raise; i.e., the interval is narrowed as much as possible.

Extra-narrowing may cause an undesirable modification in the correlation structure.

- **Condition 2.** Once $\gamma_{k|k-1}$ exceeds the minimum variation of correlation, which is recorded during the off-line simulation of a normal system operation.

Algorithm 2: [TTC] Optimized Estimation.

Input : p_i, p_j, V_i, V_j, $d_{i,j}$,$[T_{V2V}]$ and $[T_L]$.
Output: $[TTC_1]$ and $[TTC_2]$.

while *Navigation process is running* **do**
  -*Define* $[d_{i,j}]$, $[\dot{d}_{ij}]$, $[\ddot{d}_{ij}]$, $[V_i]$, $[p_i]$ *and* $[p_j]$.
  for *each couple of variables between instants* t_k *and* t_{k-1} **do**
    repeat
      -*Calculate* $C_{([X],[Y])|k}$.
      -*Estimate* $\gamma_{k|k-1}$ *(equation (17)).*
      -*Narrow the interval, if needed.*
    until *Condition 1 or 2 is satisfied*
  end
  -*Evaluate* $[TTC_1]$ *and* $[TTC_2]$ *(see equations (10) and (11))*
end

5 SIMULATION RESULTS

In this section, the reliability of the proposed interval-based models to compute the TTC is demonstrated. The quantitative results obtained from the conducted simulation are analyzed to provide a qualitative comparison between the performances of the first-order and second-order TTC formalizations.

5.1 Test Scenario and Simulation Setups

The overall set-membership TTC-based risk management is tested under a MATLAB freeway navigation simulator. Vehicle motions implicated in the test phase are simulated through the well-known tricycle kinematic model. The elaborated test scenario consists of a car-following scenario in a highway road. In addition, a model of a highway-road segment is selected as the test-scene. Otherwise, a white Gaussian noise is injected in the exact measurements of the navigation dynamics during simulation.

As already said, the follower vehicle is equipped with an ACC system. This latter exploits bounds of the interval TTC (according to the first or second-order model) to take precaution of the risk worst cases and adapt the reference distance from the vehicle ahead. Full details about the ACC operation principle are available in (Lakhal et al., 2019c).

Technically speaking, the interval computation is ensured by the reliable computation package INTLAB (Rump, 1999). All the simulation work depicted in this section is carried out under MATLAB on an Intel *i*5 Processor with 3.5 GHz and 16 GB memory. More configurations involved in the established simulation are recapitulated in Table 2.

Table 2: Simulation setups.

Parameter	Value
Sampling step	0.1 (s)
Sensors update time	0.01 (s)
Follower embedded system delay	0.025 (s)
Leader maximum velocity	22 (m/s)
Follower maximum velocity	23 (m/s)

5.2 Results and Discussion

At first, the role of the correlation analysis in providing more sharp bounds of TTC values is inspected. As shown in Figure 4, the TTC enclosures are efficiently narrowed for both $[TTC_1]$ and $[TTC_2]$. For the first-order set-membership formalization, initial amounts of uncertainties are minimized with an average range of 60.3%. Similarly, the average reduction in the width of $[TTC_2]$ due to the correlation-based optimization step is about 65.79%.

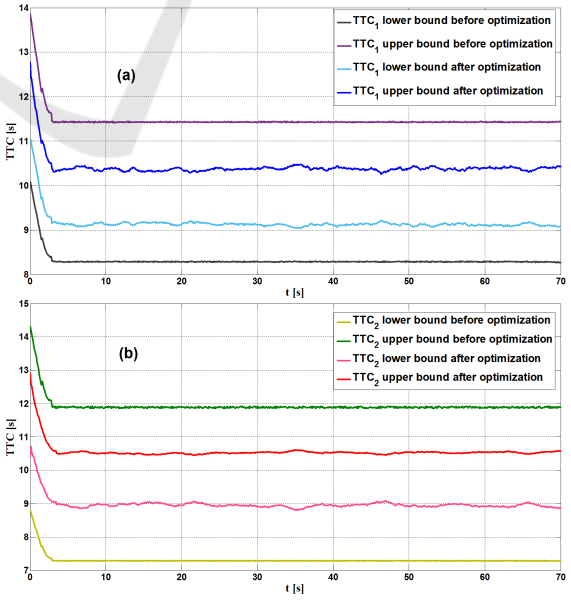

Figure 4: TTC_1 and TTC_2 enclosures with/without optimization step.

More importantly, the results of the interval high-order TTC computation model are more conservative than the low-order one. In average, the widths of $[TTC_1]$ and $[TTC_2]$ are respectively about $1.25s$ and $1.579s$. This fact can be explained by the "dependency effect" characterizing the interval arithmetic (Moore et al., 2009). Indeed, variables occurring several times in one expression are assumed as independently varying over their enclosures, which may lead to an additional pessimism in the results. Hence, more pessimism is entailed by upgrading the first-order-model to a second-order formalization since the number of the involved variables is increased.

In a second place, Figure 5 illustrates the evolution of the exact TTC_1 and TTC_2. These exact values of TTC_1 and TTC_2 are obtained in a deterministic way (respectively via equations (4) and (5)) without any noise injection during the simulation. All along the simulation run-time, the results of the two developed interval-based formalizations of the TTC enclose perfectly the reference values provided by the exact evolution of TTC_1 and TTC_2. Correspondingly, the consistency of the set-membership modeling joined with the correlation analysis is proven. Even more, the first-order interval-based TTC is more accurate than the second-one since it provides sharp bounds and simultaneously encompasses the exact and real values of the TTC. This fact optimizes implicitly the navigation traffic flow because it decreases the reference distance maintained between vehicles. Eventually, the interval-based uncertainty quantification method contributes to compensate the inaccuracy presented by the first-order TTC resulting from the modeling simplification.

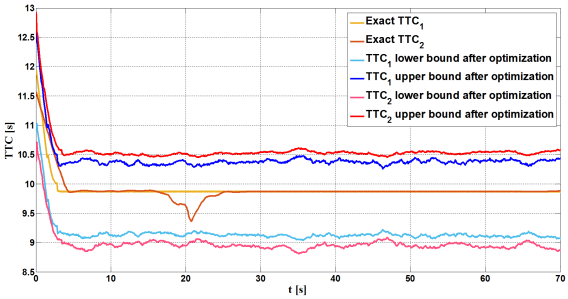

Figure 5: TTC_1 and TTC_2 enclosures compared with exact results.

Another advantage of the proposed approach is the reduction in the computational cost of the risk management of intelligent vehicles. Using simple models, which handle efficiently all possible uncertainties, helps to respect the real-time constraints. In our case of study, solving the interval quadratic polynomial to compute an over-approximation to the TTC requires $0.09s$ as an average execution time. Therefore, the TTC_1 is more efficient as a risk indicator than the TTC_2 especially in terms of computational demands. Additionally, the accuracy-level ensured by the TTC_1 is sufficient to guarantee the navigation safety since it handles properly uncertainties and modeling errors.

6 CONCLUSIONS

The reliability of models employed for the risk management of intelligent navigation systems is of utmost importance. In this work, first and second-order interval-based models to compute the TTC between two vehicles are introduced. Set-membership modeling allows considering various uncertainties and latencies that can emphasize collision risks. Moreover, the evolution of the correlation that relates variables is characterized to improve the uncertainty evaluation. Then, the performances of both proposed models are compared. The results of the first-order TTC are more compact and permit handling efficiently all uncertainties. Fast risk analysis with the same accuracy level of the second-order TTC is ensured via the simple low-order model. A trade off between accuracy and simplicity is ensured by joining the interval-based computation with correlation analysis. Accordingly, the need for sophisticated models for intelligent vehicles' motions to make the risk management successful is discarded, while mastering all uncertainty-induced risks.

Otherwise, the proposed method should be integrated in the future on a real vehicle and applied for more critical maneuvers such as lane changes.

ACKNOWLEDGEMENTS

The present work is supported by the WOW (Wide Open to the World) program of the CAP 20-25 project. It receives also the support of IMobS3 Laboratory of Excellence (ANR-10-LABX-16-01).

REFERENCES

Abdi, L. and Meddeb, A. (2018). Driver information system: a combination of augmented reality, deep learning and vehicular ad-hoc networks. *Multimedia Tools and Applications*, 77(12):14673–14703.

Ben Lakhel, N. M., Nasri, O., Gueddi, I., and Ben Hadj Slama, J. (2016). Sdk decentralized diagnosis with vertices principle component analysis. In *2016 International Conference on Control, Decision and Information Technologies (CoDIT)*, pages 517–522.

Chen, L., Yang, X., Liu, P. X., and Li, C. (2019). A novel outlier immune multipath fingerprinting model for indoor single-site localization. *IEEE Access*, 7:21971–21980.

Dey, K. C., Rayamajhi, A., Chowdhury, M., Bhavsar, P., and Martin, J. (2016). Vehicle-to-vehicle (v2v) and vehicle-to-infrastructure (v2i) communication in a heterogeneous wireless network – performance evaluation. *Transportation Research Part C: Emerging Technologies*, 68:168–184.

Fan, X., Deng, J., and Chen, F. (2008). Zeros of univariate interval polynomials. *Journal of Computational and Applied Mathematics*, 216(2):563–573.

Ferreira, J., Patrıcio, F., and Oliveira, F. (2001). A priori estimates for the zeros of interval polynomials. *Journal of Computational and Applied Mathematics*, 136(1):271–281.

Hansen, E. and Walster, G. W. (2003). *Global optimization using interval analysis: revised and expanded*, volume 264. CRC Press.

Hansen, E. R. and Walster, G. W. (2002). Sharp bounds on interval polynomial roots. *Reliable Computing*, 8(2):115–122.

Hou, J., List, G. F., and Guo, X. (2014). New algorithms for computing the time-to-collision in freeway traffic simulation models. *Computational Intelligence and Neuroscience*, 2014:1–8.

Iberraken, D., Adouane, L., and Denis, D. (2018). Multi-level bayesian decision-making for safe and flexible autonomous navigation in highway environment. In *2018 IEEE/RSJ International Conference on Intelligent Robots and Systems (IROS)*, pages 3984–3990.

Iberraken, D., Adouane, L., and Denis, D. (2019). Reliable risk management for autonomous vehicles based on sequential bayesian decision networks and dynamic inter-vehicular assessment. In *IEEE 2019 IEEE Intelligent Vehicles Symposium (IV'19)*, Paris-France.

Jaulin, L., Kieffer, M., Didrit, O., and Walter, E. (2001). *Applied Interval Analysis with Examples in Parameter and State Estimation, Robust Control and Robotics*. Springer, London.

Kasmi, A., Denis, D., Aufrere, R., and Chapuis, R. (2019). Probabilistic framework for ego-lane determination. In *2019 IEEE Intelligent Vehicles Symposium (IV)*, pages 1746–1752.

Khelifi, A., Ben Lakhal, N. M., Gharsallaoui, H., and Nasri, O. (2018). Artificial neural network-based fault detection. In *2018 5th International Conference on Control, Decision and Information Technologies (CoDIT)*, pages 1017–1022.

Lakhal, N. M. B., Adouane, L., Nasri, O., and Slama, J. B. H. (2019a). Interval-based solutions for reliable and safe navigation of intelligent autonomous vehicles. In *2019 12th International Workshop on Robot Motion and Control (RoMoCo)*, pages 124–130.

Lakhal, N. M. B., Adouane, L., Nasri, O., and Slama, J. B. H. (2019b). Interval-based/data-driven risk management for intelligent vehicles: Application to an adaptive cruise control system. In *2019 IEEE Intelligent Vehicles Symposium (IV)*, pages 239–244.

Lakhal, N. M. B., Adouane, L., Nasri, O., and Slama, J. B. H. (2019c). Risk management for intelligent vehicles based on interval analysis of ttc. *IFAC-PapersOnLine*, 52(8):338–343. 10th IFAC Symposium on Intelligent Autonomous Vehicles IAV 2019.

Lozenguez, G., Adouane, L., Beynier, A., Martinet, P., and Mouaddib, A. I. (2011). Map partitioning to approximate an exploration strategy in mobile robotics. In *PAAMS 2011, 9th International Conference on Practical Applications of Agents and Multi-Agent Systems*, Salamanca-Spain.

Moore, R., Kearfott, R., and Cloud, M. (2009). *Introduction to Interval Analysis*. Society for Industrial and Applied Mathematics.

Nasri, O., Lakhal], N. M. B., Adouane, L., and Slama], J. B. H. (2019). Automotive decentralized diagnosis based on can real-time analysis. *Journal of Systems Architecture*, 98:249 – 258.

Nicola, J. and Jaulin, L. (2018). *Comparison of Kalman and Interval Approaches for the Simultaneous Localization and Mapping of an Underwater Vehicle*, pages 117–136. Springer International Publishing, Cham.

Rigatos, G. G. (2012). Nonlinear kalman filters and particle filters for integrated navigation of unmanned aerial vehicles. *Robotics and Autonomous Systems*, 60(7):978–995.

Rump, S. (1999). INTLAB - INTerval LABoratory. In Csendes, T., editor, *Developments in Reliable Computing*, pages 77–104. Kluwer Academic Publishers, Dordrecht.

Wang, S., Wang, W., Chen, B., and Tse, C. K. (2018). Convergence analysis of nonlinear kalman filters with novel innovation-based method. *Neurocomputing*, 289:188–194.

Ward, J. R., Agamennoni, G., Worrall, S., Bender, A., and Nebot, E. (2015). Extending time to collision for probabilistic reasoning in general traffic scenarios. *Transportation Research Part C: Emerging Technologies*, 51:66–82.

Wu, Y., Wei, H., Chen, X., Xu, J., and Rahul, S. (2020). Adaptive authority allocation of human-automation shared control for autonomous vehicle. *International Journal of Automotive Technology*, 21(3):541–553.

Xia, B., Shang, Y., Nguyen, T., and Mi, C. (2017). A correlation based fault detection method for short circuits in battery packs. *Journal of Power Sources*, 337:1 – 10.

Yang, W., Wan, B., and Qu, X. (2020). A forward collision warning system using driving intention recognition of the front vehicle and v2v communication. *IEEE Access*, 8:11268–11278.

Zhang, M. and Deng, J. (2013). Number of zeros of interval polynomials. *Journal of Computational and Applied Mathematics*, 237(1):102 – 110.